ELSEVIER

Systematic variation of interfacial phase reactivity in dental nanocomposites

Kristen S. Wilson[a],*, Kai Zhang[a,b], Joseph M. Antonucci[a]

[a]*Polymers Division, National Institute of Standards and Technology, 100 Bureau Drive, MS 8545, Gaithersburg, MD 20899, USA*
[b]*Polymer Research, Zimmer, Inc., Warsaw, IN 46580, USA*

Abstract

This study was designed to determine the effect of varying the chemistry of the interfacial phase on critical composite properties in dental nanocomposite materials. Silica nanoparticles were silanized with varying ratios of 3-methacryloxypropyltrimethoxysilane (MPTMS) and octyltrimethoxysilane (OTMS) while keeping the total amount of silane constant at 10% by mass fraction relative to the mass of filler. The silanized nanoparticles were mixed into a dimethacrylate resin (60% filler by mass fraction). The mechanical properties of the uncured pastes were assessed by compression testing between parallel plates. The composites were photo-cured and tested by biaxial flexure and three-point bend flexure testing. Fracture surfaces were analyzed by field-emission scanning electron microscopy (FE-SEM). At maximized filler mass fractions, the workabilities of the uncured pastes were better maintained as the fraction of OTMS in the interphase increased relative to MPTMS. The flexure strengths and moduli of the MPTMS silanized and dual silanized composites were similar but decreased as OTMS mass fractions in the silane mixture increased to 7.5% and 10%. FE-SEM images revealed evidence for phase separation in the composites containing silica silanized with high fractions of OTMS. Among the potential practical benefits of dual silanized nanoparticles are the improved workability of composite pastes with higher filler loadings that should lead to higher modulus composites with lower polymerization shrinkage.
Published by Elsevier Ltd.

1. Introduction

Thermoset methacrylate-based composites are being used increasingly as direct polymeric dental restorative materials because their chemical, physical, and mechanical properties are adequate for many dental applications. In addition, they have excellent aesthetic qualities, and they have relatively high cure efficiency in free radical photo-polymerization [1–3]. However, the hostile oral environment with its chemical, physical, biochemical, and thermal challenges, and the high masticatory loads encountered by dental restoratives, especially in posterior teeth, necessitate further property improvements in these materials. Specifically, more durable composites with improved strength and modulus, better control of the polymerization process leading to high degrees of vinyl conversion, low water sorption, improved processability, and low polymerization shrinkage are needed [4–9].

The essential phases of most polymeric dental restorative materials are the matrix, filler, and interphase. The matrix, or continuous phase, is typically derived from the monomer system that includes a free radical initiating system. The filler or dispersed phase is designed to enhance the modulus of the softer polymer phase and usually consists of glass or ceramic particles of different compositions, sizes, and size distributions. Dental composites containing nanosized fillers reflect the growing interest in the dental community in nanostructured restorative materials. The interphase,

*Corresponding author. Tel.: +1 301 975 8091;
fax: +1 301 975 4924.
E-mail address: wilson_kristen@hotmail.com (K.S. Wilson).

probably the least understood of the composite phases, is typically derived from organosilanes and is designed to chemically bind to the matrix and the filler phases. Although the filler–matrix interphase is the least abundant phase (by mass) of the composite material, it can have significant effects on the properties of composites. In the case of nanocomposites, the interphase plays an even more important role, since the nanoparticle fillers have an extremely high surface area-to-volume ratio and require a higher degree of silanization than larger particulate fillers.

In this study, the chemistry of the silica nanoparticle–matrix interphase was systematically altered by silanizing a pure nanosized silica with a reactive silane that can copolymerize with the polymer network (3-methacryloxypropyltrimethoxysilane-MPTMS), a non-reactive silane that does not copolymerize (n-octyltrimethoxysilane-OTMS), or various blends of these two silanes (dual silanization). Dual silanized fillers have a number of potential advantages. Since water sorption continues to be a concern in the field of dental materials, the hydrophobic nature of the OTMS may help prevent water sorption and subsequent hydrolytic degradation of the interphase and, therefore, increase the lifetime of the materials in the oral environment [6]. Also, recent studies have shown that non-reactive silanes may benefit dental composites by reducing polymerization stress [10]. The aim of this research was to better understand the structure–property relationships of silane surface chemistries resulting from dual silanization of silica nanoparticle fillers by assessing the effects of various silane-generated interfacial phases on uncured composite paste workability, degree of vinyl conversion upon photo-polymerization, modulus, biaxial flexural strength, and the morphology of the thermoset methacrylate composites.

2. Experimental

2.1. Material selection

All the materials used in this study, 2,2-bis[p-(2′-hydroxy-3′-methacryloxypropoxy)-phenyl] propane (BisGMA), triethyleneglycol dimethacrylate (TEGDMA) (both monomers from Esstech, Essington, PA), Aerosil OX50 fumed amorphous silica (Degussa, Dublin, OH), MPTMS, OTMS (both from Gelest, Inc., Tullytown, PA), cyclohexane (J.T. Baker, Phillipsburg, NJ), n-propylamine, ethyl 4-dimethylaminobenzoate (4E), and camphorquinone (CQ) (all from Aldrich, Milwaukee, WI) were used as received without further purification. According to the manufacturer, Aerosil OX50 silica had an average particle diameter of 40 nm, with the particle size distribution ranging from 10 nm up

Table 1
Mass fractions of MPTMS and OTMS used for silanizing the silica nanoparticles relative to the mass of silica

MPTMS (% mass fraction)	OTMS (% mass fraction)
10	0
7.5	2.5
5	5
2.5	7.5
0	10

to 80 nm in diameter, and a surface area of $50\,m^2g^{-1} \pm 15\,m^2g^{-1}$.

2.2. Silanization of silica nanoparticles

The Aerosil OX50 silica nanoparticles were silanized using a previously reported procedure [14]. The powders were silanized with different ratios of MPTMS and OTMS as shown in Table 1. In all cases, the total amount of organosilane was kept constant at 10% by mass fraction relative to silica. Previous studies conducted in our laboratories suggested that 10% silane by mass fraction was more than enough to completely cover the surface of the silica and to provide a durable interphase. The fact that the chosen amount of silane was enough to coat the particles was verified using the following equation:

$$X = (A/\omega)f,$$

where X is the amount of silane (g) needed to coat the silica, A is surface area of the silica ($50\,m^2g^{-1}$), ω is the surface area coverage per gram of silane ($2525\,m^2g^{-1}$) assuming each silane molecule covered $1.11\,nm^2$ [15,16], and f is the amount of silica (g). According to this equation, assuming that MPTMS and OTMS both covered the same amount of surface area per gram of silane, 5.0 g of OX50 silica required 0.1 g of silane (only 2% silane by mass fraction) for minimum uniform coverage. Therefore, the amount of silane used in this study was more than enough.

A representative procedure for the silanization of silica is described. The silica powder (5.0 ± 0.05 g) was weighed into a 250-mL round bottom flask. Cyclohexane (100 mL), n-propylamine (0.1 ± 0.01 g), and the silane(s) (0.55 ± 0.01 g) were subsequently added to the flask. The mixture was stirred at room temperature for 30 min and then at $60 \pm 5\,°C$ for an additional 30 min at atmospheric pressure. The mixture was placed under a moderate vacuum (≈ 2.7 kPa) using a rotary evaporator at $60 \pm 5\,°C$ until the solvent and volatile byproducts were removed (≈ 15 min). The dried powder was then heated at $95 \pm 5\,°C$ for 1 h under the same vacuum on a rotary evaporator. Finally, the powder was dried at $80\,°C$ in a vacuum oven (≈ 2.7 kPa) for 18 h.

2.3. Composite preparation

The resin for the polymer phase was prepared by mixing BisGMA and TEGDMA (50:50 by mass fraction) followed by heating at $60 \pm 0.5\,^{\circ}$C for approximately 30 min or until the mixture was homogeneous. The photo-initiating reagents, 4E (0.8% mass fraction) and CQ (0.2% mass fraction), were added to the resin which was heated in the dark at $60 \pm 0.5\,^{\circ}$C until the photo-initiator components were dissolved in the monomer mixture. The silanized silica powders (60% mass fraction) were mixed into the photo-activated resin by hand spatulation. Once the powders were completely wetted with resin, the composite pastes were sheared against a glass surface with a Teflon spatula until the pastes were semi-translucent to assure optimal particle dispersion quality. Composites containing unsilanized silica (50% mass fraction) were prepared and used as a control. The lower concentration of unsilanized silica in the control samples was necessary because the hydrophilic nature of the particles prevented concentrations any higher than 50% mass fraction. At concentrations above 50% mass fraction of unsilanized silica, the uncured composites were dry, crumbly, and unworkable.

2.4. Characterization of physical and mechanical properties

The mechanical properties of the uncured composite pastes were measured under compression between parallel plates using an EnduraTEC ELF 3200 testing instrument. Composite pastes containing 60% and 66% silanized silica by mass fraction were tested. The mass fraction of 66% silanized silica was chosen to represent samples in which the amount of silica had been maximized. These pastes were prepared with no photo-initiator to prevent changes in properties upon exposure to ambient light. For each compression test, 1.00 ± 0.02 g of the paste was molded into a cylindrical shape approximately 7.5 mm in height and 11 mm in diameter on a Teflon sheet (0.16 mm thick) and a second Teflon sheet was placed on top of the paste. Placement of the Teflon sheets in this manner minimized friction during sample compression. The paste was first compressed with parallel plates between the Teflon sheets at $1\,\text{mm}\,\text{s}^{-1}$ to 6 mm in height and then compressed at $0.05\,\text{mm}\,\text{s}^{-1}$ to 2 mm in height. Stress–strain data for the paste compression between 6 and 2 mm were calculated ($n = 3$). A "compression modulus" for each paste was obtained from the slope of the stress–strain curve at maximum strain. A more detailed description of this test procedure will be described in a future publication.

The degree of conversion (DC) was measured using a Thermo Nicolet Nexus 670 Fourier Transform Infrared (FTIR) Spectrometer (Madison, WI) equipped with OMNIC 6.1 software. The composite pastes were pressed into plastic molds (2 ± 0.2 mm thick × 13 mm ± 0.2 mm in diameter) between two glass slides and cured for 1 min per side using a Dentsply Triad 2000 light-curing system at a wavelength of 470 nm (York, PA). Spectra were taken in the near-IR region (7500–4000 cm^{-1}) and 64 scans were taken per sample before and after curing. DC was calculated by comparing the area under the C$=$C band at 6170 cm^{-1} before and after photo-curing ($n = 5$). The peak areas were normalized with respect to sample thickness [11]. Near-IR analyses at 23 $^{\circ}$C were conducted immediately (less than 1 min) after curing and again 24 h after curing. During the 24 h period, the cured composites were stored at room temperature and were not exposed to ambient light.

Mechanical tests on cured composites were conducted using a computer-controlled Universal Testing Machine model 5500R (Instron Corp., Canton, MA) operated by Testworks4 software. Composite specimens were stored in distilled water at $37 \pm 0.5\,^{\circ}$C for 24 h prior to mechanical testing according to procedures established in the literature [12,13]. The values reported are the average of 5–7 specimens and the error bars indicate the standard deviations. Moduli and flexure strengths were determined for the composite specimens using a three-point bend test geometry. The specimens were 2 ± 0.2 mm thick and 2 ± 0.2 mm wide and were tested with a 20 mm span at a crosshead speed of $0.5\,\text{mm}\,\text{min}^{-1}$. Biaxial flexural strength (BFS) values were determined for composite disks 15 ± 0.2 mm in diameter and 1.3 ± 0.2 mm thick at a crosshead speed of $0.5\,\text{mm}\,\text{min}^{-1}$.

Scanning electron microscopy images of the composite fracture surfaces were obtained using a field-emission scanning electron microscope (FE-SEM, Hitachi 4700) operating at 2 kV. The fracture surfaces were sputter-coated with gold for fifteen seconds prior to analysis (expected gold layer thickness ≈ 2.5 nm).

In this paper, the error bars and $\pm$ symbols correspond to one standard deviation and are taken as an estimate of the standard uncertainty. Statistical differences between sample data were determined using the two-tailed student's t-test at a 95% confidence interval.

3. Results

For clarity, the composites described herein will be abbreviated according to the type of silane surface treatment used on the silica nanoparticles. For example, a composite filled with silica silanized with 10% MPTMS will be referred to as the "10 M composite" and a composite filled with silica silanized with 5% MPTMS and 5% OTMS will be referred to as the

"5M:5O composite". The silanized silica particles will likewise be identified with these acronyms.

3.1. Mechanical properties of uncured composite pastes

The silica nanoparticle-filled composite pastes were prepared by mixing the silanized silica powders into the resin by hand with a Teflon spatula followed by shearing against a glass surface with the spatula. During this process, it was observed that variations in the silane interfacial chemistry caused obvious differences in how readily the silica could be mixed into the resin, and in the final texture and workability of the pastes. The tactile quality of dental composite pastes is a real issue for dentists who tend to prefer cohesive pastes that can be easily manipulated into small crevices of the tooth structure and do not stick to dental tools.

A range of paste textures was observed that depended upon both the silane interfacial chemistry and the mass fraction of silanized silica in the paste. In the samples containing 60% silanized silica (60% S), the 10M paste behaved like a sticky, extremely viscous fluid, the 7.5M:2.5O and 5M:5O pastes were both cohesive and less sticky than the 10M paste, and the 2.5M:7.5O and 10O pastes were non-cohesive, thick, and creamy in texture. The pastes containing 66% silanized silica (66% S) represented samples in which the mass fraction of silica had been maximized. The 66% S samples were all fairly cohesive, wax-like materials in which the degree of pliability increased as the amount of OTMS increased.

To quantitatively assess differences in the workability of the pastes, the responses of the pastes under compression between Teflon-lined parallel plates were measured for 60% S and 66% S pastes. The stress–strain curves for the two sets of samples highlighted the significant effect of interfacial chemistry variations on the material properties of the pastes (Fig. 1). The "modulus" of each paste was determined from the slope of the stress–strain curve at high strain and these values

Table 2
"Modulus" (MPa) of uncured composite pastes containing 60% or 66% silanized silica by mass fraction under compression between parallel plates

Silane type	60% silanized silica	66% silanized silica
10M	0.067	0.742
7.5M:2.5O	0.119	0.743
5M:5O	0.154	0.611
2.5M:7.5O	0.208	0.500
10O	0.224	0.492

are shown in Table 2. For the 60% S pastes, the "modulus" steadily increased as the silane interface changed from purely MPTMS to purely OTMS. The 66% S pastes all had higher moduli than the 60% S pastes; however, the MPTMS to OTMS trend was generally reversed. The only exception in the 66% S trend was that the 7.5M:2.5O paste had a slightly higher "modulus" than the 10M paste.

The "compression modulus" data elucidated the fact that variations in silica surface chemistry and the subsequent changes in particle–particle and particle–matrix interactions had a significant effect on the ability to increase the mass fraction of silica in the pastes. Hydrogen bonding and dipole forces between the 10M silica and the resin as well as interparticle interactions caused the modulus of the paste to increase sharply as the mass fraction of 10M silica in the pastes increased from 60% S (0.067 MPa) to 66% S (0.742 MPa). The 10O silica, however, possessed an aliphatic interphase that allowed the particles to blend into the resin without participating in strong hydrogen bonding interactions such that the "modulus" of the paste increased less sharply as the mass fraction of 10O silica increased from 60% S (0.224 MPa) to 66% S (0.492 MPa). The dual silanized silica particles all behaved in a manner intermediate between the 10M and 10O particles in which the hydrogen bonding and dipole interactions evolving from the MPTMS were tempered by the weaker interactions of the OTMS.

In terms of uncured paste texture and workability, it was determined that dual silanized (MPTMS and OTMS) silica provided certain advantages. At a concentration of 60% S, the pastes containing dual silanized silica were more cohesive than the 10M and 10O pastes, and therefore better suited for practical use by dental professionals. Also, the dual silane system permitted higher mass fractions of filler while maintaining paste workability (at least up to 66% S) as confirmed by their lower "compression moduli" compared to 10M pastes. The increased mass fraction of filler is important for enhancing the modulus of cured composites and reducing cure shrinkage.
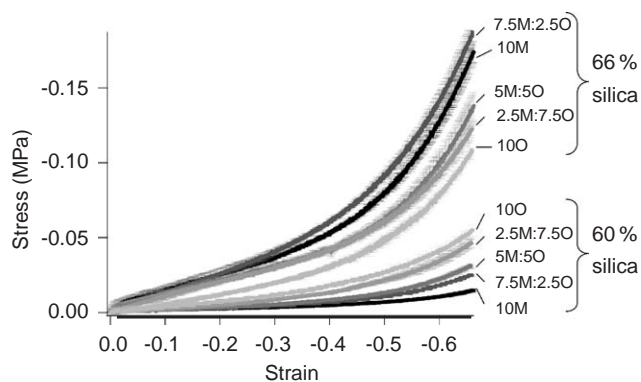

Fig. 1. Stress-strain curves for uncured composite pastes containing 60% and 66% silanized silica by mass fraction analyzed under compression between parallel plates ($n = 3$).

3.2. Methacrylate conversion

DCs for composites containing 60% silanized silica by mass fraction, 50% unsilanized silica by mass fraction, and the unfilled resin were measured using near-IR and the data are shown in Fig. 2. The DCs immediately after curing for the 7.5M:2.5O, 5M:5O, 2.5M:7.5O, and the unsilanized silica composites were statistically the same (approximately 74% conversion). In comparison, the 10M composite had a significantly lower conversion ($72.0 \pm 0.3\%$) while the unfilled resin and the 10O composite displayed statistically significant increases in DC up to $76.0 \pm 0.7\%$ ($p < 0.05$). Twenty-four hours after curing, the DC increased for all composite specimens. The highest DC ($82.3 \pm 0.2\%$) was measured for the 10O composite.

In general, the DCs reported for the nanocomposites in this study were comparable to conversions reported for other dental composite materials [6,8,17,18]. The data obtained 24 h after curing indicated that DC increased slightly with time due to significant post-cure polymerization. These data indicated that some of the unreacted methacrylate groups within the network had enough mobility to continue to react for up to 24 h. Twenty-four hours after curing, the DCs for the 7.5M:2.5O, 5M:5O, and 2.5M:7.5O composites were the same as the unfilled copolymer networks, suggesting that the 40 nm silica particles at this concentration in the resin did not inhibit conversion. In the 10M composite, it is expected that the dense packing of methacrylate groups on the surface of the silica caused the slightly lower DC. The MPTMS-silanized nanoparticles, with their greater concentration of vinyl groups, may have acted more like multifunctional monomers, causing

gelation to occur at lower conversions and thereby limiting the DC. In contrast, the DC for the 10O composites after 24 h was statistically greater than the other composites and the unfilled network. This increased conversion may have been caused by a plasticizing effect in which the non-reactive, organically modified silica particles acted like a non-reactive diluent that increased the mobility of the dimethacrylate monomers in the growing polymer networks and resulted in enhanced vinyl addition.

3.3. Mechanical properties of cured composites

The mechanical properties of composites containing 60% silica by mass are summarized in Table 3. It was determined that the BFS of the 5M:5O composite was not significantly different from the 10M composite ($p > 0.05$) but was significantly greater than the 7.5M:2.5O composite ($p < 0.05$). The 2.5M:7.5O and 10O composites displayed BFS values significantly lower than the other three composites. The three-point bend test provided both flexure strength and modulus data for each composite. The three point bend flexure strength of the 10M, 7.5M:2.5O, and 5M:5O composites were all statistically the same ($p > 0.05$) and the flexure strengths of the 2.5M:7.5O and 10O composites were significantly lower than the others as well as significantly different from each other. The moduli for the composites were all statistically similar (approximately 5800 MPa) except for the 10O composite that had a significantly lower modulus (4229 ± 161).

The BFS data showed that the highest flexure strength values were obtained for the 10M, 7.5M:2.5O, and 5M:5O composites and that the 5M:5O composite displayed higher flexure strength than the 7.5M:2.5O composite. From these data, it was concluded that the highest coverage of methacrylate groups at the silica–matrix interphase was not necessary to obtain high flexure strength. However, when the interphase contained less than 5% MPTMS surface coverage

% Methacrylate Conversion
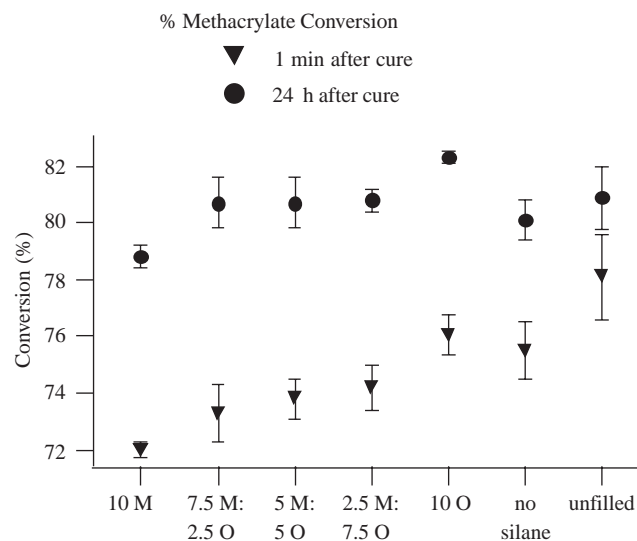▼ 1 min after cure
● 24 h after cure

Fig. 2. Near-IR conversions for composites containing 60% silanized silica by mass, 50% unsilanized silica by mass, and the unfilled polymer approximately 1 min after curing and 24 h after curing.

Table 3
Mechanical properties of the composites 24 h after photo-polymerization

Composite	BFS (MPa)	Flexure strength (MPa)	Modulus (MPa)
Unsilanized	63 (27)	43 (11)	5478 (727)
10M	127 (19)	80 (13)	5863 (209)
7.5M:2.5O	117 (17)	90 (15)	5827 (223)
5M:5O	156 (23)	87 (10)	5792 (374)
2.5M:7.5O	92 (3)	60 (11)	5365 (290)
10O	59 (9)	33 (4)	4230 (161)

The flexure strength and modulus were obtained by three-point bend testing. "Unsilanized" refers to the composite that contained 50% unsilanized silica by mass fraction. The silanized composites contained 60% silica by mass. Standard deviations are shown in parentheses.
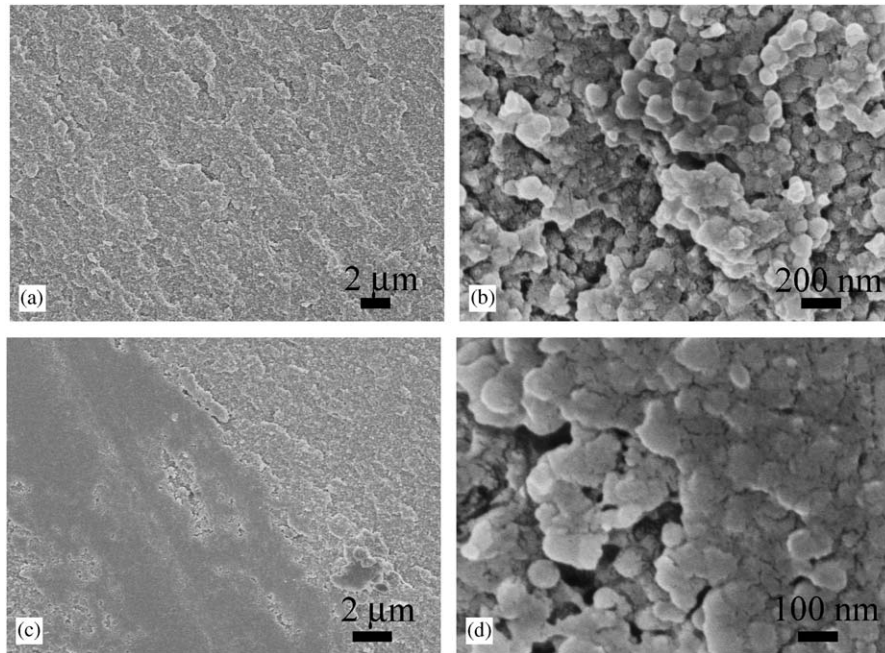
Fig. 3. FE-SEM images of 10M composite fracture surfaces (a) a representative region, (b) high magnification of a representative region, (c) a sporadic dark region, and (d) high magnification of the dark region. The dark regions appeared to be areas where the composite fracture surface was very flat. Silica particles were visible in this region.

(2.5M:7.5O and 10O composites), the flexure strength decreased significantly. Since it was unlikely that the MPTMS methacrylate groups copolymerized to full conversion with the resin, this BFS data highlighted the fact that only a fraction of covalent linkages between the filler and polymer matrix phase were important for maintaining high composite strengths. The three-point bend flexure data confirmed these results.

The three-point bend data revealed that the interfacial phase had no measurable effect on the modulus of the composites, except in the case of the 10O composite. In order to investigate the reason for the lower modulus of the 10O composite, the composite fracture surfaces were analyzed by FE-SEM. Images of a 10M composite fracture surface are shown in Fig. 3. These surfaces appeared to be mostly homogeneous, rough surfaces in which the silica particles were evenly distributed. Some dark regions were visible, however, and upon closer inspection these dark regions appeared to be areas where the fracture surfaces were abnormally flat. Silica particles were clearly seen in these regions in concentrations qualitatively similar to the rougher composite regions. Similar flat areas were seen in the 7.5M:2.5O and 5M:5O composites. Images of 2.5M:7.5O and 10O composite fracture surfaces are shown in Fig. 4 and these surfaces were generally homogeneous and rough. These images highlight some irregularly shaped dark areas that were seen periodically scattered on the surfaces. These regions were markedly different in composition compared to the dark regions in the 10M,

7.5M:2.5O, and 5M:5O composites. At high magnifications, a distinct boundary was observed between the composite phase (light region) and polymer phases that did not appear to be filled with silica (dark region). It was proposed that these pockets of low-modulus, polymer-rich phases behaved like defects and contributed to the lower modulus of the bulk 10O composite material. In the 2.5M:7.5O composite, the polymer phases may have slightly lowered the modulus, but not enough to make a significant difference.

One possible explanation for the pockets of polymer-rich phases was that the particles were poorly dispersed prior to curing the composites. Particle dispersion quality was a function of several factors, including the balance between particle–particle and particle–matrix attractive and repulsive forces. In the 10O and 2.5M:7.5O pastes, poor dispersion quality might have occurred if the attractive interparticle van der Waals forces were greater than the interactions between the silanized particles and the BisGMA/TEGDMA matrix. The MPTMS-treated silica particles, however, were likely to be more thermodynamically stable and better dispersed in the uncured resin because the hydrogen bonding and dipole interactions between the particles and the resin would have helped overcome interparticle attractive forces.

A second explanation is that the OTMS-silanized silica particles, which did not covalently bond with the resin, were effectively forced out of the polymer network during photo-polymerization, resulting in
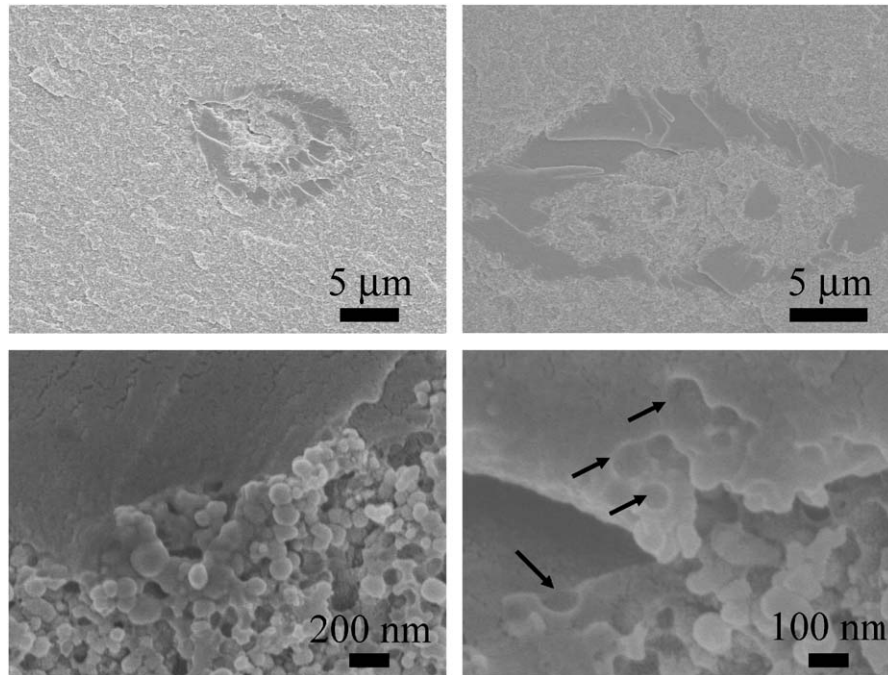
Fig. 4. FE-SEM images of fracture surfaces (a) 2.5M:7.5O composite showing sporadic dark region, (b) 10O composite showing sporadic dark region, (c) 10O composite at high magnification focused on the boundary between the light and dark regions, and (d) high magnification of 10O composite at the border of the dark region. The dark regions in the 7.5M:2.5O and 10O composite correspond to polymer-rich zones containing little or no visible silica. There is a clear boundary between the composite phase and the unfilled polymer-rich phase as seen in (c). The black arrows indicate holes in the polymer-rich phase where particles appeared to have been plucked out.

phase separation. Polymerization-induced phase separation is a phenomenon in which the increasing molecular mass of a polymer network in a mixed or blended system during polymerization causes thermodynamic instabilities that are overcome by phase separation of the immiscible components. This is a process that has been well established in the field of liquid crystal–polymer composites [19,20]. In this study, the 10O composites contained a high mass fraction of filler relative to polymer and so the phase separation manifested itself as micrometer-sized polymer-rich zones in a "continuous phase" of the polymer–particle composite. The major thermodynamic contribution to the attractive force between the OTMS-silanized particles was van der Waals interactions. In the cases where MPTMS was present on the surface of the silica, it was proposed that the formation of covalent bonds between the particles and the polymerizing network as well as hydrogen bonding interactions with the network inhibited significant phase separation. Although the 2.5M:7.5O particles contained MPTMS in their interphase, the 2.5M:7.5O composites showed evidence of phase separation. In this case, the concentration of co-polymerizing MPTMS groups within the interphase may have been insufficient to prevent phase separation.

4. Discussion

The aim of this study was to develop an understanding of the effect of interfacial surface chemistry in dental nanocomposites on critical composite properties. Nanoparticle fillers of the type represented by OX50 have traditionally been used in relatively small quantities as co-fillers along with larger sized fillers. The advantages of using nanoparticles in hybrid-type composites are that these thixotropic particles prevent filler settling and can "fill in" the regions between the larger particles, allowing for larger volume fractions of filler and reducing polymerization shrinkage. To obtain high volume fractions of silica nanoparticles in dental resins, the particle surface chemistry must be optimized.

In this study, composites containing only nanoparticle fillers were considered so that a fundamental understanding of the nanocomposite structure–property relationships could be developed. To achieve this goal, a series of silica particles were silanized with tailored surface chemistries designed to interact differently with the resin matrix. MPTMS (a difunctional silane typically used in silica-reinforced dental materials) provided covalent linkages between the particles and the matrix and also interacted with the resin through hydrogen bonding. The methacrylate group of MPTMS reacted

with the resin during photo-polymerization and the silyl ether group reacted with the silanol groups of silica during the silanization procedure. OTMS, however, did not react with the methacrylate monomers by copolymerization but only interacted through weak van der Waals forces. Nanocomposites containing silica silanized with blends of these two chemically different silanes displayed some interesting properties. Future work will be directed towards determining the mechanical properties of composites prepared using a maximum amount of dual silanized silica fillers of different types and sizes. Also, polymerization shrinkage and polymerization stress of these types of composites will be measured along with their methacrylate conversions and mechanical properties.

5. Conclusions

The implication of this research was that dual silanization using blends of MPTMS and a non-reactive silane such as OTMS was a facile method for improving the workability of composite pastes. Using dual silanized filler interphases, up to 66% silanized silica by mass could be incorporated into the resin while maintaining good paste workability. Also, it was determined that the mechanical properties of the 7.5M:2.5O and 5M:5O composites were comparable to those of the 10M composites.

Dual silanized silica nanoparticles are expected to make excellent co-fillers in hybrid composite materials. Their optimized surface chemistry will allow for higher mass fractions of filler phase and, therefore, may reduce polymerization shrinkage compared to hybrid systems containing only MPTMS-silanized particles. Also, the dual silanized particles have the potential to alter interfacial properties, for example, by reducing water sorption because of the increased hydrophobicity derived from the hydrocarbon octyl silane, and also possibly reducing polymerization stress due to the greater flexibility of OTMS compared to MPTMS.

Disclaimer

Certain commercial materials and equipment are identified in this article to specify the experimental procedure. In no instance does such identification imply recommendation or endorsement by the National Institute of Standards and Technology or that the material or equipment identified is necessarily the best available for the purpose.

References

[1] Antonucci JM. New monomers for use in dentistry. In: Gebelein CG, Koblitz FF, editors. Biomedical and dental applications of polymers. New York: Plenum; 1981. p. 357–71.

[2] Antonucci JM, Stansbury JW. Molecularly designed dental polymers. In: Arshady R, editor. Desk reference of functional polymers. Washington, DC: American Chemical Society; 1997. p. 719–38.

[3] Moszner N, Salz U. New developments of polymeric dental composites. Prog Polym Sci 2001;26:535–76.

[4] Kalachandra S, Taylor DF, DePorter CD, Grubbs HJ, McGrath JE. Polymeric materials for composite matrices in biological environments. Polymer 1993;34:778–82.

[5] Kalachandra S, Sankarapandian M, Shobha HK, Taylor DF, McGrath JE. Influence of hydrogen bonding on properties of Bis-GMA analogues. J Mater Sci: Mater Med 1997; 8:283–6.

[6] Sideridou I, Tserki V, Papanastasiou G. Study of water sorption, solubility and modulus of elasticity of light-cured dimethacrylate-based dental resins. Biomaterials 2003;24:655–65.

[7] Ferracane JL, Antonio RC, Matsumoto H. Variables affecting the fracture toughness of dental composites. J Dent Res 1987;66:1140–5.

[8] Halvorson RH, Erickson RL, Davidson CL. The effect of filler and silane content on conversion of resin-based composite. Dent Mater 2003;19:327–33.

[9] Xu HHK, Quinn JB, Smith DT, Antonucci JM, Schumacher GE, Eichmiller FC. Dental resin composites containing silica-fused whiskers: effects of whisker-to-silica ratio on fracture toughness and indentation properties. Biomaterials 2002;23:735–42.

[10] Condon JR, Ferracane JL. Reduced polymerization stress through non-bonded nanofiller particles. Biomaterials 2002;23:3807–15.

[11] Stansbury JW, Dickens SH. Determination of double bond conversion in dental resins by near infrared spectroscopy. Dent Mater 2001;17:71–9.

[12] Mitsuhashi A, Hanaoka K, Teranaka T. Fracture toughness of resin-modified glass ionomer restorative materials: Effect of powder/liquid ratio and powder particle size reduction on fracture toughness. Dent Mater 2003;19:747–57.

[13] Xu HHK, Smith DT, Schumacher GE, Eichmiller FC, Antonucci JM. Indentation modulus and hardness of whisker-reinforced heat-cured dental resin composites. Dent Mater 2000;16:248–54.

[14] Chen TM, Brauer GM. Solvent effects on bonding organo-silane to silica surfaces. J Dent Res 1982;61:1439–43.

[15] Liu Q, Ding J, Chambers DE, Debnath S, Wunder SL, Baran GR. Filler-coupling agent-matrix interactions in silica/poly-methylmethacrylate composites. J Biomed Mater Res 2001;57:384–93.

[16] Soderholm KJM, Shang SW. Molecular orientation of silane at the surface of colloidal silica. J Dent Res 1993; 72:1050–4.

[17] Ferracane JL. Current trends in dental composites. Crit Rev Oral Biol Med 1995;6:302–18.

[18] Khatri CA, Stansbury JW, Schultheisz CR, Antonucci JM. Synthesis, characterization and evaluation of urethane derivatives of Bis-GMA. Dent Mater 2003;19:584–8.

[19] Nwabunma D, Chiu HW, Kyu T. Morphology development and dynamics of photopolymerization-induced phase separation in mixtures of a nematic liquid crystal and photocuratives. Macro-molecules 2000;33:1416–24.

[20] Rajaram CV, Hudson SD, Chien LC. Morphology of polymer-stabilized liquid crystals. Chem Mater 1995;7:2300–8.